

A critical view on the deeply bound K^-pp system

April 14, 2019

V.K. Magas¹, E. Oset², A. Ramos¹ and H. Toki³

¹ Departament d'Estructura i Constituents de la Matèria,
Universitat de Barcelona, Diagonal 647, 08028 Barcelona, Spain

² Departamento de Física Teórica and IFIC Centro Mixto
Universidad de Valencia-CSIC, Institutos de Investigación de Paterna
Apdo. correos 22085, 46071, Valencia, Spain

³ Research Center for Nuclear Physics, Osaka University,
Ibaraki, Osaka 567-0047, Japan

Abstract

We briefly review the situation around the claimed deeply bound K^- states in different recent experiments and concentrate particularly on the state K^-pp seen by the FINUDA collaboration in nuclear K^- absorption. We perform a theoretical simulation of the process and show that the peak in the Λp spectrum that was interpreted as a deep K^-pp bound state corresponds mostly to the process $K^-pp \rightarrow \Lambda p$ followed by final state interactions of the produced particles with the remnant nucleus.

1 Introduction

The theoretical predictions of deeply bound pionic atoms [1–3], which were observed in the (d , ${}^3\text{He}$) [4, 5], following suggestion of the theoretical studies of [6, 7], have stimulated the search for bound states of different hadrons in nuclei. One of the natural continuations was the study of K^- bound states. The large potential used at that time [8] to reproduce existing data on K^- atoms fed the ideas that deeply bound K^- states (bound by 50–200 MeV) could exist. The question, of course, arises, as to whether the widths of the states are narrow enough to distinguish between neighboring states. One should distinguish these deeply bound states from other states bound by a few MeV in heavy nuclei that different realistic potentials predict and which have not yet been observed [9–12].

A step forward in the theoretical description of the K^- nucleus optical potential was given in [13] establishing a link between the optical potential and the presence of the

$\Lambda(1405)$ resonance, which, in free space, appears 27 MeV below the K^-p threshold. In the medium, the effect of Pauli blocking on the excitation of intermediate $\bar{K}N$ states demanded more energy to have the same phase space, as a consequence of which the $\Lambda(1405)$ was produced at higher energies. Correspondingly, the zero in the real part of the in-medium K^-p amplitude appears above the K^-p threshold and, as a consequence, the repulsive free-space K^-p amplitude at threshold turns into an attractive one in the medium.

The effect described above remains in all present theoretical works as the driving mechanism to get an attractive K^- nucleus optical potential. Yet, the fact that the K^- feels an attractive selfenergy in the medium facilitates the generation of the $\Lambda(1405)$ at smaller energies, moving the zero of the amplitude back to smaller energies and, eventually, ending up below the K^-N threshold leading again to repulsion. It becomes clear at this point that a selfconsistent calculation is needed, and it was done in [14] where a small attraction was finally found with the resonance position barely modified.

Subsequent improvements introducing also the selfenergy of the pions and the baryons was done in [15] by means of which a potential was obtained that reproduced the data for the K^- atoms [11]. This potential, which automatically accounts for new many body decay channels with respect to former ones, like $K^-NN \rightarrow \Sigma N$, ΛN , $\Sigma^* N$, leads to deeply bound states with $B \approx 30$ MeV, but the width of the states is around 100 MeV [11]. Potentials with the same strength when selfconsistency is imposed are found in [15–17].

With this behavior for the $\bar{K}N$ dynamics in nuclei having been established, the claim given in [18] on the possible existence of narrow deeply bound states in $A = 3, 4$ nuclei, predicting a $A = 3$, $I = 0$ state with a binding energy of 100 MeV, was surprising. The situation became more puzzling when an experiment searching for deeply bound K^- states found a signal for a strange tribaryon [19] which was claimed not to correspond to the state predicted in [18], since its interpretation as a bound state would imply a binding energy around 200 MeV and the state had $I = 1$. Subsequent corrections of the potential in [20] involving some spin-orbit effects and relativistic corrections (which had been accounted for in other works [15, 16]), plus some extra ad hoc modifications, could lead to the extra binding of the kaon, as a consequence of which the findings of [19] have been lately presented as evidence of deeply bound K^- atoms [21, 22].

In a recent paper [23] two of us make a critical review of the theoretical works [18, 20] and also of the interpretation of the peak in the experiment of [19]. The main criticisms raised in [23] are the following. The theoretical potential in [18, 20] eliminates the direct coupling of $\pi\Sigma \rightarrow \pi\Sigma$ and $\pi\Lambda \rightarrow \pi\Lambda$ in contradiction with the results of chiral theory that establishes large couplings for them [24]. This assumption prevents the finding of two $\Lambda(1405)$ states as appears recently in all chiral unitary approaches for the $\bar{K}N$ system [25–29] and which gets experimental support from the study of the $K^-p \rightarrow \pi^0\pi^0\Sigma^0$ reaction [30] done in [31]. The experimental $\Lambda(1405)$ resonance, which is a superposition of these two states, is assumed in [18, 20] to be a bound state of $\bar{K}N$, contradicting the results of the chiral theories and leading to a $\bar{K}N$ amplitude in $I = 0$ twice as large below the K^-p threshold. The selfconsistency shown to be essential in [14, 15, 32] is not implemented in [18, 20] and, finally, the system is allowed to shrink to densities as large as 10 normal nuclear densities, $\rho = 10\rho_0$, at the center of the nucleus resulting into a deeper K^- nucleus potential. With

all these assumptions and approximations, the potential of [20] has a strength of about a factor twenty larger than that of the chiral approach. Furthermore, the work of [18, 20] does not take into account the many body decay channels considered in [15] and, as was shown in [23], had them been taken into account, and with the densities claimed in [18, 20], the width of the K^- state should have been of the order of 200 MeV or higher, instead of the width of about 20 MeV assumed in [18, 20].

Convinced by these arguments that the peak found at KEK [19] could not correspond to a deeply bound K^- state, the authors of [23] searched for other explanations and found a natural mechanism that passed all tests. The peak is due to the reaction $K^-NN \rightarrow \Sigma p$ in ${}^4\text{He}$ leaving the other nucleons as spectators. Such an interpretation demanded the peak corresponding to the reaction $K^-NN \rightarrow \Lambda p$ be seen as well, which was indeed the case in the experiment. This latter peak disappeared when a cut for “fast” pions was done (the pions coming from Λ decay have momentum in the range 61 – 196 MeV/c) and was prominent in the complementary cut of “slow pions”. The interpretation demanded that the peaks had to be seen in other nuclei, a test also passed by the FINUDA data presented in [33]. In addition, the requirement that the daughter nucleus is just a spectator becomes more difficult in heavier nuclei since the distortion of the Λ or p particle in their way out through the nucleus leads unavoidably to nuclear excitations. As a consequence of this, one expects the signals to fade gradually for heavier nuclei, which is also a feature of the FINUDA data.

With the situation of the KEK experiment clarified, the reanalysis of the interpretation of the FINUDA data, leading to a claim of a bound state of K^-pp by 115 MeV, is an absolute necessity and this is the purpose of the present work.

The FINUDA collaboration in [34] looks for Λp events back to back following the K^-pp absorption in ${}^6\text{Li}$, ${}^7\text{Li}$ and ${}^{12}\text{C}$ nuclei. A narrow peak in the invariant mass is observed, which is identified with $K^-pp \rightarrow \Lambda p$ removing just the binding energy. This implicitly assumes ground state formation of the daughter nucleus since nuclear excitations lead necessarily to a broad peak, namely the quasielastic peak. On the other hand, a broad second peak of about 60 MeV width, which is identified in [34] as a signal for the K^-pp bound state, is seen at smaller Λp invariant masses and of much larger strength than the first peak. In the present work we shall see that this peak, with its strength, position, width and angular dependence corresponds to the same two-nucleon absorption mechanism discussed above, but leading to nuclear excitation, which has a much larger strength than the fraction leading to the ground state in the daughter nucleus.

To reach the former conclusion, a computer simulation calculation is made allowing the stopped kaons in the nucleus to be absorbed by a pair of nucleons of a local Fermi sea. The nucleon and the Λ emitted in the $K^-pp \rightarrow \Lambda p$ and $K^-pn \rightarrow \Lambda n$ absorption processes are allowed to rescatter with other nucleons in the nucleus leading to nuclear breakup and producing a nucleon spectrum with a distinct peak corresponding to one collision. This peak, which is analogous to the quasielastic peak of any inclusive reaction like (e, e') , (π, π') , (p, p') etc, reproduces the experimental peak taken in [34] as a signal of the K^-pp bound state. Another peak, broader and at smaller energies coming from baryon secondary collisions, also appears both in our simulation and in the experimental data at the same

place and hence, an explanation for the whole experimental spectrum is found, which does not require to invoke the creation of the K^-pp bound state.

2 The theoretical framework

The results of [34] are presented for a mixture of data from ${}^6\text{Li}$, ${}^7\text{Li}$ and ${}^{12}\text{C}$. We shall perform the calculations for ${}^{12}\text{C}$, but we consider the presence of the other nuclei when needed. The reaction is



with stopped kaons. The Λp events are collected and, as done in the experiment, two cuts are made: one selecting $p_\Lambda > 300 \text{ MeV}/c$, to eliminate events from $K^- p \rightarrow \Lambda \pi$, and another one imposing $\cos \Theta_{\vec{p}_\Lambda \vec{p}_p} < -0.8$, to filter Λp pairs going back to back.

The K^- absorption at rest proceeds by capturing a slow K^- in a high atomic orbit of the nucleus, which later cascades down till the K^- reaches a low lying orbit, usually the first state in light nuclei, where it finally gets absorbed by the nucleus. The cut $p_\Lambda > 300 \text{ MeV}/c$ in the experiment allows us to neglect the one body $K^- N \rightarrow \Lambda \pi$ reaction and concentrate exclusively on the two body absorption mechanism.

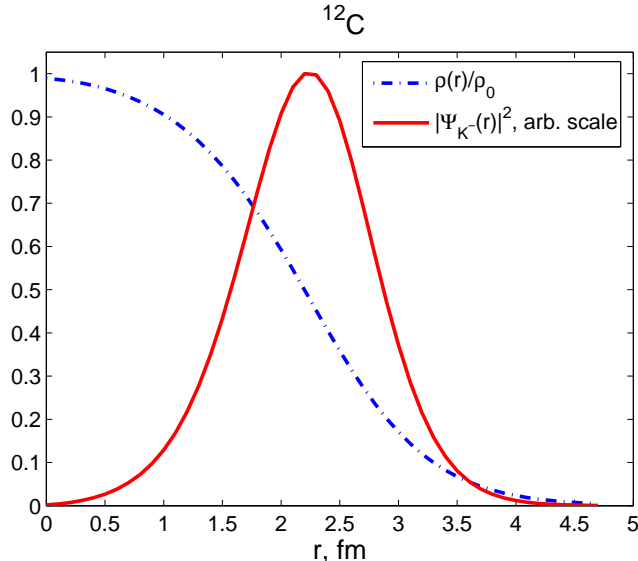


Figure 1: Nuclear density profile for ${}^{12}\text{C}$ and corresponding $|\Psi_{K^-}(\vec{r})|^2$ defined by Eq. (2).

For the purpose of the absorption reaction explored in this paper, the K^- wave function, $\Psi_{K^-}(\vec{r})$, requires only, as a basic feature, to peak around the surface of the nucleus. This is technically implemented by assuming it to be proportional to the derivative of the nuclear density. We therefore take

$$|\Psi_{K^-}(\vec{r})|^2 \sim |d\rho(r)/dr|^2, \quad (2)$$

where $\rho(r)$ is the nuclear density, see Fig. 1.

The K^- absorption width from pN pairs in a nucleus with A nucleons is proportional in first approximation to the square of the nuclear density [35] multiplied by the probability

of finding the K^- in the nucleus, hence, it is given by the expression:

$$\begin{aligned}\Gamma_A &= \text{Norm} \int d^3\vec{r} |\Psi_{K^-}(\vec{r})|^2 \left(\frac{\rho(r)}{2}\right)^2 \sigma_m \\ &= \text{Norm} \int d^3\vec{r} |\Psi_{K^-}(\vec{r})|^2 2 \int \frac{d^3\vec{p}_1}{(2\pi)^3} \Theta(k_F(r) - |\vec{p}_1|) 2 \int \frac{d^3\vec{p}_2}{(2\pi)^3} \Theta(k_F(r) - |\vec{p}_2|) \\ &\quad \times \sigma_m(\vec{p}_1, \vec{p}_2, \vec{p}_K, \vec{r}) ,\end{aligned}\quad (3)$$

where we have used $\rho(r) = 4 \int \frac{d^3\vec{p}_1}{(2\pi)^3} \Theta(k_F(r) - |\vec{p}_1|)$ for the nucleons with momenta \vec{p}_1, \vec{p}_2 in the Fermi sea, k_F is the Fermi momentum at the local point, Θ is the step function, Norm is a proportionality constant that has dimensions of R^7 and $\sigma_m(\vec{p}_1, \vec{p}_2, \vec{p}_K, \vec{r})$ is the in-medium cross section for the $K^- pN \rightarrow \Lambda N$ process given by

$$\begin{aligned}\sigma_m(\vec{p}_1, \vec{p}_2, \vec{p}_K, \vec{r}) &= \int \frac{d^3\vec{p}_\Lambda}{(2\pi)^3} \frac{M_\Lambda}{p_\Lambda^0} \int \frac{d^3\vec{p}_N}{(2\pi)^3} \frac{M_N}{p_N^0} (2\pi)^4 \delta^4(p_\Lambda + p_N - p_1 - p_2 - p_K) \\ &\quad \times \overline{\sum_{s_i} \sum_{s_f}} |T_{K^- pN \rightarrow \Lambda N}|^2 \Theta(|\vec{p}_N| - k_F(r)) ,\end{aligned}\quad (4)$$

where $\vec{p}_K, \vec{p}_\Lambda, \vec{p}_N$ are momenta of the corresponding particles, and $\overline{\sum_{s_i} \sum_{s_f}} |T_{K^- pN \rightarrow \Lambda N}|^2$ will be assumed to be approximately constant for $\vec{p}_K = 0$, and $|\vec{p}_1|, |\vec{p}_2| \ll M$.

Now we insert eq. (4) into eq. (4), perform the integration over $d^3\vec{p}_1$ and the angular part of $d^3\vec{p}_2$, and absorb all the constants into Norm:

$$\begin{aligned}\Gamma_A &= \text{Norm} \int d^3\vec{r} |\Psi_{K^-}(\vec{r})|^2 \int \frac{d^3\vec{p}_\Lambda}{p_\Lambda^0} \int \frac{d^3\vec{p}_N}{p_N^0} \int dp_2 p_2 \frac{p_\Lambda^0 + p_N^0 - p_2^0 - m_K}{|\vec{P}|} \\ &\quad \times \Theta\left(k_F(r) - \sqrt{|\vec{P}|^2 + |\vec{p}_2|^2 - 2|\vec{P}||\vec{p}_2|A}\right) \Theta(k_F(r) - |\vec{p}_2|) \Theta(|\vec{p}_N| - k_F(r)) \Theta(1 - A^2) ,\end{aligned}\quad (5)$$

where $\vec{P} = \vec{p}_\Lambda + \vec{p}_N$, and A provides the cosine of the angle between \vec{P} and \vec{p}_N ,

$$A \equiv \cos \Theta_{\vec{P}\vec{p}_N} \equiv \frac{M^2 + \vec{P}^2 + \vec{p}_2^2 - (p_\Lambda^0 + p_N^0 - p_2^0 - m_K)^2}{2|\vec{P}||\vec{p}_2|} .\quad (6)$$

In order to take into account the propagation of the produced nucleon and Λ through the nucleus after K^- absorption we insert a kernel $K(\vec{p}, \vec{r})$ into eq. (5) for both particles. This kernel has been used in Monte Carlo simulations of pion nucleus reactions [36], proton nucleus reactions [37], electron nucleus reactions [38], leading to good reproduction of inclusive cross sections and selected channels of one and two nucleon emission, etc. Thus the final expression for the K^- absorption width from pN pairs in nucleus A is given by

$$\begin{aligned}\Gamma_A &= \text{Norm} \int d^3\vec{r} |\Psi_{K^-}(\vec{r})|^2 \int \frac{d^3\vec{p}_\Lambda}{p_\Lambda^0} \int \frac{d^3\vec{p}_N}{p_N^0} \int dp_2 p_2 \frac{p_\Lambda^0 + p_N^0 - p_2^0 - m_K}{|\vec{P}|} \\ &\quad \times \Theta\left(k_F(r) - \sqrt{|\vec{P}|^2 + |\vec{p}_2|^2 - 2|\vec{P}||\vec{p}_2|A}\right) \Theta(k_F(r) - |\vec{p}_2|) \Theta(|\vec{p}_N| - k_F(r)) \Theta(1 - A^2) \\ &\quad \times K(\vec{p}_\Lambda, \vec{r}) K(\vec{p}_N, \vec{r}) .\end{aligned}\quad (7)$$

The procedure accomplished by eq. (7) is the following. A kaon at rest is absorbed from the surface of the nucleus by two nucleons (pp or pn) whose momenta are chosen randomly from the local Fermi sea, with a Fermi momentum $k_F(r) = (3\pi^2\rho(r)/2)^{1/3}$, where $\rho(r)$ is the experimental nuclear density. Energy and momentum conservation is demanded according to phase space and hence two momenta of the emitted p (n) and Λ are generated. The primary nucleon is allowed to rescatter with nucleons in the nucleus by means of

$$\begin{aligned} pN &\rightarrow p'N' \\ np &\rightarrow pn \quad (\text{fast } n \text{ to fast } p) \end{aligned} \tag{8}$$

according to a probability per unit length given by $\sigma\rho(r)$, where σ is the experimental NN cross section at the corresponding energy. The Λ is allowed to scatter similarly, assuming a cross section of $\sigma_{\Lambda N} \equiv \frac{2}{3}(\sigma_{pN} + \sigma_{nN})$, which is a reasonable choice based on the observation that realistic YN potentials predict a Λ mean-field potential depth in nuclei of about 2/3 that of the nucleon [39]. The nucleons from the Fermi sea that participate in the collisions are also chosen randomly, the variables of the scattering particles are boosted to their Center of Mass (CM) frame, an angular distribution is generated according to experiment (for ΛN it is assumed to be the same as for NN) and a boost back to the Lab frame is performed. After several possible collisions, one or more nucleons and a Λ emerge from the nucleus and the invariant mass of all possible Λp pairs, as well as their relative angle, are evaluated for each Monte Carlo event and stored conveniently to generate the required histograms.

3 Formation of the ground state of the final daughter nucleus

In order to make the discussion simple, we are going to take the ${}^7\text{Li}$ nucleus, one of those used in FINUDA experiment and likely the candidate (like the others) to produce the narrow peak in the Λp invariant mass spectrum of [34]. The process under consideration would be

$$K^- {}^7\text{Li} \rightarrow p \Lambda {}^5\text{H}. \tag{9}$$

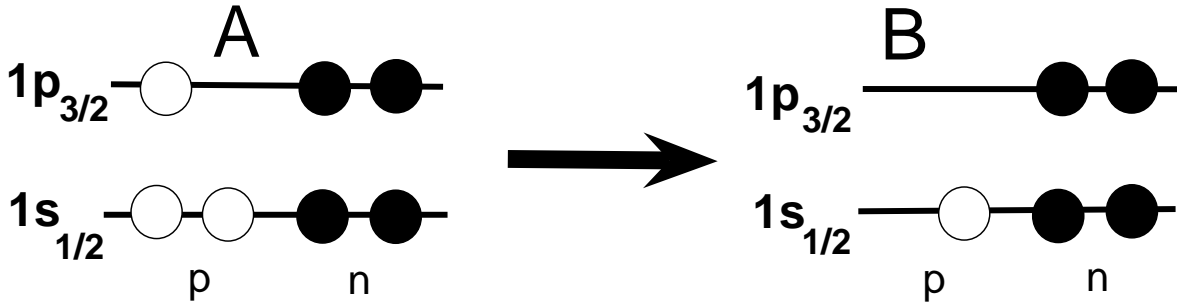


Figure 2: A) The ground state of ${}^7\text{Li}$; B) The ground state of ${}^5\text{H}$.

A simple shell model structure of ${}^7\text{Li}$ is given in Fig. 2a. In the same picture the ground state (g.s.) of the daughter nucleus after the removal of two protons would be given by Fig. 2b. It is clear that even if ${}^5\text{H}$ had an approximate structure like in Fig. 2b, its orbitals are different from those of the ${}^7\text{Li}$, which means that the overlap of the corresponding wave functions is smaller than 1:

$$| < \Psi_{{}^5\text{H}}(\text{gs}) | \Psi_{{}^7\text{Li}}(\text{gs})(pp)^{-1} > | < 1 . \quad (10)$$

Actually, for the discussion that follows, we do not need to know the precise value of this overlap. Values for it of the order of 0.5 – 0.7 are already large, which would lead to a formation probability, defined as

$$\text{Form. prob.} = | < \Psi_{{}^5\text{H}}(\text{gs}) | \Psi_{{}^7\text{Li}}(\text{gs})(pp)^{-1} > |^2 , \quad (11)$$

of the order or smaller than 0.3. The formation probability is a concept used in α decay, where such an overlap plays an important role in the decay rates when four particles are removed from the father nucleus [40].

The formation probability is not all what matters in the reaction. In α decay one has to consider the probability of penetrating through the potential barrier. In the present case the formation probability has to be weighted by the “survival probability”, corresponding to the situation in which both the p and the Λ cross the daughter nucleus without any collision. This is so because any such collision would excite the nucleus, which would then not be in its ground state. By looking at Fig. 3 one observes that, for the K^- being absorbed on the surface, only one baryon (p or Λ) will cross the nucleus, and the survival probability will be

$$P_s = e^{- \int_0^\infty \sigma \rho(\vec{r}') dl} , \quad (12)$$

where $\vec{r}' = \vec{r} + l \vec{p}/p$ and $\sigma \simeq 20$ mb for 581 MeV/c, corresponding to the momentum of the proton coming from $K^- pp \rightarrow p\Lambda$ absorption. Such an estimate gives $P_s \simeq 0.4$, which is confirmed by the more accurate value of $P_s = 0.395$ extracted from our Monte Carlo simulations. Combining this factor with the formation probability of ≤ 0.3 , we finally estimate a 10% probability for having the remnant nucleus in its ground state after a $K^- pp$ absorption event. Although crude, the former evaluation of the role of the g.s. formation is sufficient for our purposes, since all we need to know is that the largest part of the strength following K^- absorption in nuclei goes to nuclear excitations.

It should also be mentioned here that the possibility of removing two protons from the s-wave orbit in Fig. 2 leading to a final ${}^5\text{H}$ excited nucleus in the continuum without further interaction of the p or Λ is negligible due to small overlap between these two states. This means in practice that the excitation of the nucleus will require the secondary collision of the p or Λ after the $K^- pp$ absorption process.

In Fig. 3 of [34] a narrow peak is observed around $\sqrt{s} = 2340$ MeV, already interpreted by the authors as the g.s. formation process described above. A question arises then: if this process accounts for only a small fraction of the absorption rate, where does the bulk of it go in the experiment of [34]? Obviously this strength will go into the region of smaller

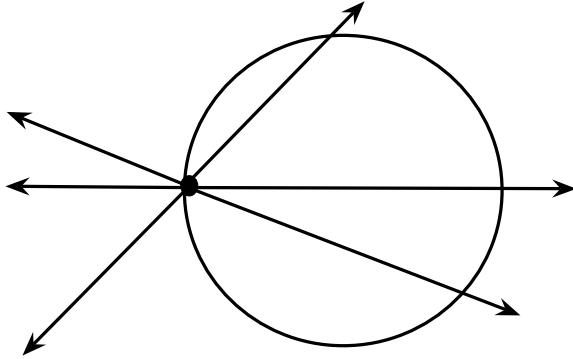


Figure 3: A simplified K^- absorption picture for the estimation of the survival probability.

invariant Λp mass and one can immediately guess that the broad peak to the left of the narrow peak in the spectrum of Fig. 3 of [34] will account for these events. To check this hypothesis we present in the next section the distribution of strength for the events in which the emitted particles following K^- absorption undergo collisions in their way out of the remnant nucleus, after having applied the same cuts in the Λ momentum and the Λp relative angle as in the experiment [34].

4 Spectrum of the secondary collisions

The spectrum of secondary collisions is generated from our computer simulation algorithm of eq. (7) which allows the particles emitted after K^- absorption to re-scatter in their way out of the residual nucleus. The nucleons move under the influence of a mean field potential which we take to be given by the Thomas-Fermi expression:

$$V(r) = -\frac{k_F(r)^2}{2m_N}. \quad (13)$$

However, the removal energy of two protons is only about 30 MeV with this model, while the actual removal energy to create the g.s. of the daughter nucleus is about 50 MeV. The Thomas-Fermi model implies no gap for nuclear excitation, whereas the problem we are facing suggests a gap of about 8 – 10 MeV. This is easily implemented into our theoretical framework imposing the potential of eq. (13) for the unoccupied states, and the same potential minus 8 MeV for the occupied states of the Fermi sea.

The results of the calculated spectrum with just one collision after K^- absorption are shown in Fig. 4. Checking the thick line, which corresponds to the sum of the two possible absorption mechanisms, $K^- pp$ and $K^- pn$, with final state interactions (FSI), one can see a bump in the spectrum, which peaks around the same position and is somewhat broader than the main peak of Fig. 3 of [34]. Since we measure the Λp invariant mass the main contribution comes from $K^- pp \rightarrow \Lambda p$ absorption. The contribution from the $K^- pn \rightarrow \Lambda n$ reaction followed by $np \rightarrow pn$ is represented in the figure by the dotted line. We can see

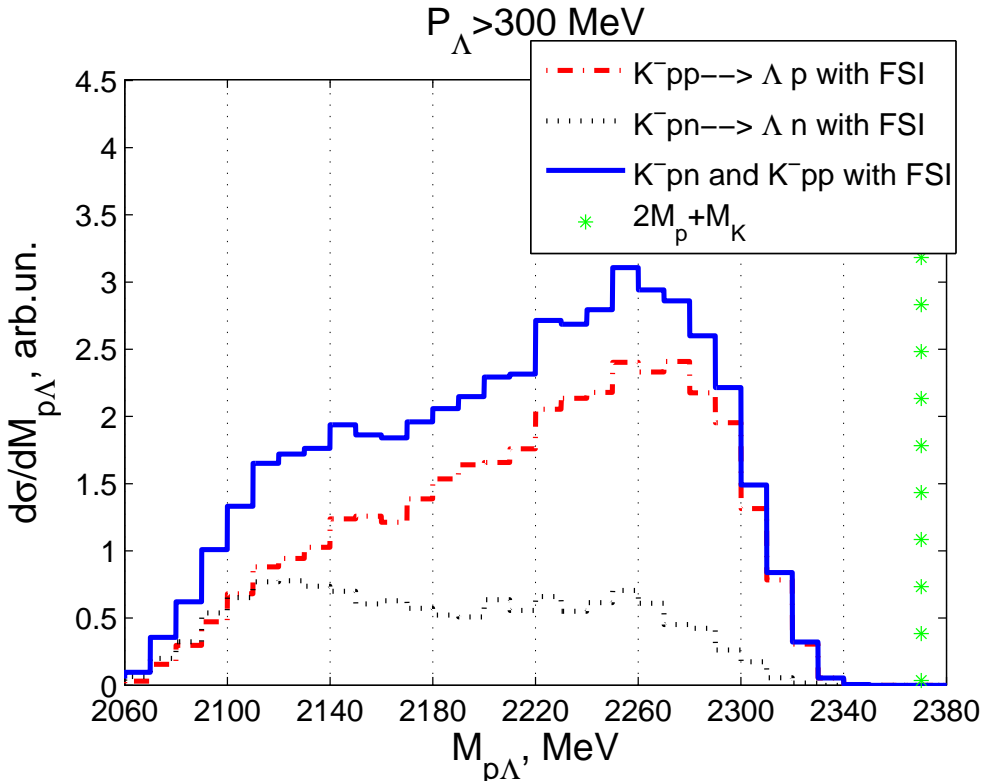


Figure 4: Invariant mass of Λp distribution for K^- absorption in ^{12}C with maximum one collision of the outgoing particles with the daughter nucleus.

that in the most interesting region, $\sqrt{s} = 2260 - 2300$ MeV, this process contributes by only about 20 %, while in the lower invariant mass region it becomes as important as the $K^-pp \rightarrow \Lambda p$ reaction. Low invariant masses correspond to the situation of Λp pairs with a low energy proton kicked above Fermi sea in a collision with the primary nucleon. We will see below that the amount of such events will increase when we allow more than one secondary collision. Most of such events are, of course, not back to back and will be removed when implementing the experimental angle cut.

The angular distribution of the Λp events is shown in Fig. 5, where we have added to the spectrum with secondary collisions the strength of the peak corresponding to the g.s to g.s. transition, which has been imposed to be about 10% according to the arguments given in the previous section. In our simulations, the g.s. to g.s. reaction corresponds to the case of no secondary collisions. We observe that the angular dependence of the peak for a transition to the g.s. of the daughter nucleus is obviously back to back, since the three particles participating in the absorption mechanism are practically at rest. Even assuming that the K^-pp system gets about 200 MeV/c momentum from the Fermi motion of the protons, this only leads to 4 MeV recoil energy for the daughter nucleus, making the Λp system move with velocity given as $200\text{MeV}/(m_K + 2m_p)$, and the angle between Λ and p fulfills $\cos \Theta_{\vec{p}_\Lambda \vec{p}_p} < -0.95$. Thus, all events of K^- absorption contributing to the narrow peak in the FINUDA experiment fall within the experimental cuts.

As we can see, the angular distribution of the total strength in Fig. 5 peaks backward as in the experiment (see Fig. 2 of [34]).

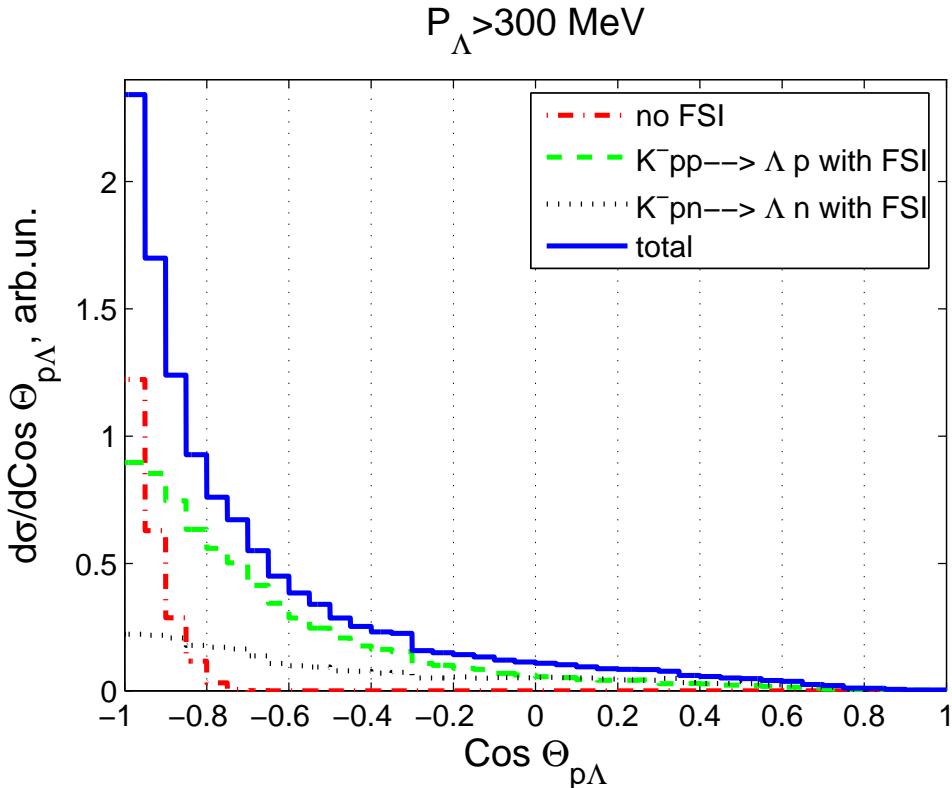


Figure 5: Opening angle distribution between a Λ and a proton for the same simulation as in Fig. 4. For the no final state interaction curve (no FSI), which corresponds to the g.s to g.s. transition, we assumed the 10% probability for having the remnant nucleus in its ground state after a K^-pp absorption event.

Next we impose the experimental restrictions in our calculated spectrum. Since the cut $p_\Lambda > 300$ MeV/c is eventually fulfilled by almost all absorption events, it is already imposed in all the figures shown. On the other hand, the back to back angle cut, $\cos \Theta_{\vec{p}_\Lambda \vec{p}_p} < -0.8$, has a substantial effect, as can be seen in Fig. 6, narrowing considerably the invariant Λp mass spectrum, which looks now much more similar to the one in Fig. 3 of [34].

We can go further by allowing further collisions of the proton or Λ . In Figs. 7 and 8 we show, respectively, the spectrum of the Λp invariant mass without and with the experimental angle cut, and allowing up to three collisions of the Λ or p particles with the nucleons in the Fermi sea of the daughter nucleus. The spectrum develops a second bump around $\sqrt{s} = 2160$ MeV, which is actually also present in the experimental data [34].

We have thus seen how the experimental spectrum is naturally explained in our Monte Carlo simulation of the K^- absorption events in nuclei, without the need of exotic mechanisms like the formation of a K^-pp bound state.

5 Further mechanisms

In this section, we explore other possible reactions which could also produce some strength in the region of energies addressed in the figures.

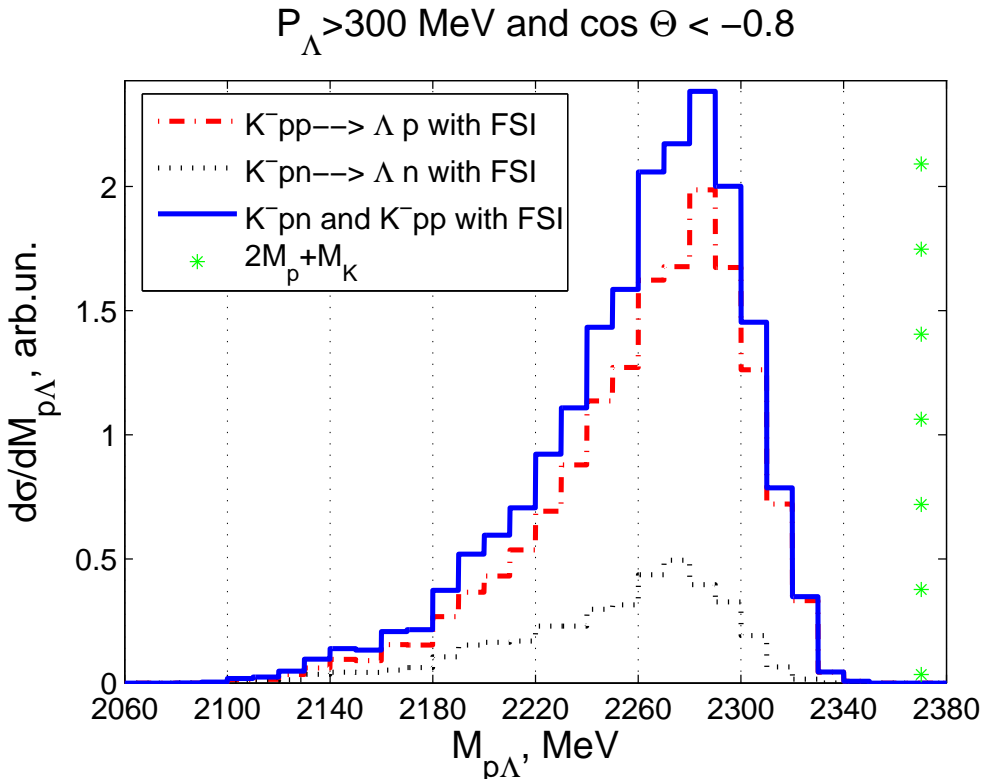


Figure 6: The same as Fig. 4, but imposing the experimental angle cut for back to back events, $\cos \Theta_{\vec{p}_\Lambda \vec{p}_p} < -0.8$.

We start discussing the mechanism $K^- pp \rightarrow \Sigma^0 p$ followed by $\Sigma^0 \rightarrow \Lambda \gamma$, mentioned in [34] and discarded there with the claim “however, the observed invariant mass distribution is too broad to be attributed to this process only”.

It is easy to check the kinematics by combining relativistically the momenta of the p from $K^- pp \rightarrow \Sigma^0 p$ and the Λ from $\Sigma^0 \rightarrow \Lambda \gamma$ and one obtains that the strength of this channel goes in the Λp invariant mass region between $\sqrt{s} = 2200$ MeV and $\sqrt{s} = 2265$ MeV and that all events fulfill the relative angle condition. With respect to the strength of this mechanism, we note that, according to the experimental findings of K^- absorption in ${}^4\text{He}$ [41], there is a fraction of 11.7 % for combined K^- absorption leading to $\Lambda(\Sigma^0)pnn$. This fraction is split into 2.3 % for Σ^0 and 9.4 % for Λ using arguments of isospin symmetry. Given the fact that isospin symmetry is badly broken at threshold [24], a different estimate was done in [23] providing a ratio of Λ to Σ^0 production of the order of one. For the estimates we assume an average between these two values, accepting large uncertainties, and we take $R = \Gamma(\Lambda p)/\Gamma(\Sigma^0 p) \approx 2$. Assuming now a fraction for the g.s. formation of the daughter nucleus similar for the two processes, there would be only about ~ 5 % of the K^- absorption width going to $\Sigma^0 p + \text{g.s.}$ followed by necessity by the $\Lambda \gamma$ (the main decay mode of the Σ^0). Therefore, even if the events fall within the relevant energy range, the strength of this mechanism is too small to have a significant effect in the main peak.

We consider now the K^- absorption events that go to $\Sigma^0 p$ followed by some collision of the p or Σ^0 , with final $\Sigma^0 \rightarrow \Lambda \gamma$ decay as before. The fact that the Σ^0 and p have originally smaller momentum than the Λ and p in the $K^- pp \rightarrow \Lambda p$ absorption has as a

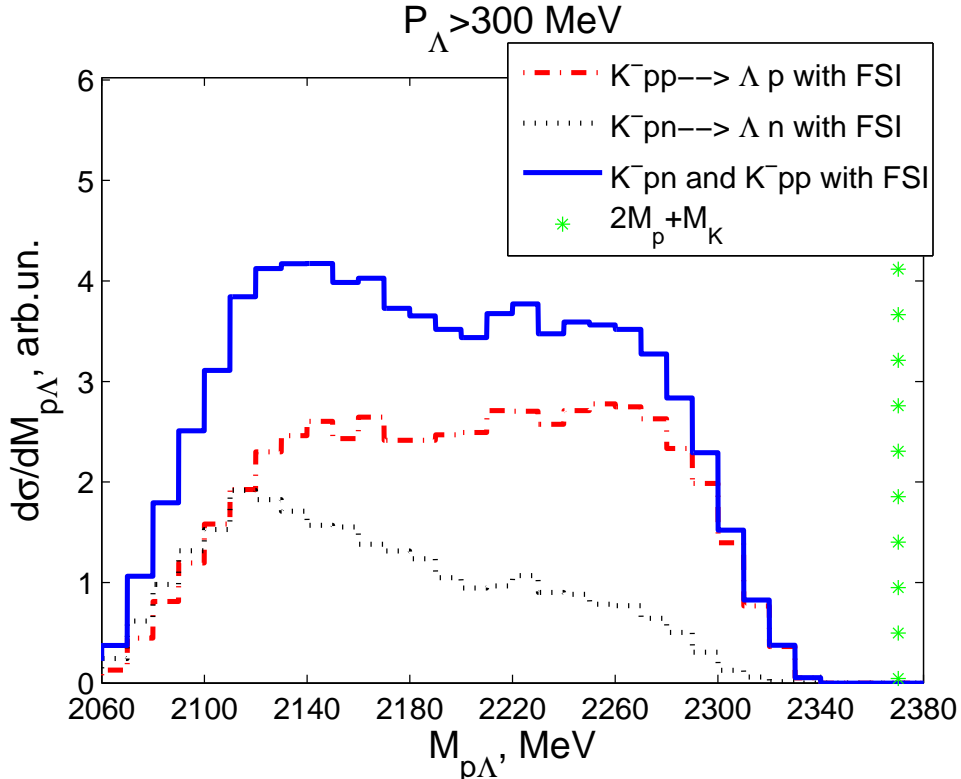


Figure 7: Invariant mass of Λp distribution for K^- absorption in ^{12}C allowing up to three collisions of the outgoing particles with the daughter nucleus.

consequence that fewer collisions overcome Pauli blocking and bigger collision angles are required to overcome it. This, together with the Λ momentum relative to the Σ^0 , makes very small the fraction of events that fulfill the experimental condition $\cos \Theta_{\vec{p}_\Lambda \vec{p}_p} < -0.8$. A simple calculation shows that assuming $R = 2$, only a fraction of about 10 % of the big peak in Fig. 3 of [34] can come from this process, and these filtered events concentrate around $\sqrt{s} = 2250$ MeV.

Another source of Λp pairs to be investigated is the chain reaction $K^- NN \rightarrow \Sigma N_1$ followed by $\Sigma N_2 \rightarrow \Lambda p$, with N_2 a nucleon from the Fermi sea. We can have

$$\begin{aligned}
 K^- pp &\rightarrow \Sigma^+ n; \quad \Sigma^+ n \rightarrow \Lambda p \\
 K^- pp &\rightarrow \Sigma^0 p; \quad \Sigma^0 p \rightarrow \Lambda p \\
 K^- pn &\rightarrow \Sigma^0 n; \quad \Sigma^0 p \rightarrow \Lambda p
 \end{aligned} \tag{14}$$

According to [41] the combined rate for the three Σ formation reactions shown in the left column of eq. (14) would be 3.3 % versus 9.9 % for Λp formation. If we take the ratio of Λ to Σ^0 production to be $R = 2$, as discussed earlier, the numbers would be 4.9 % versus 7.8 %. Therefore, roughly speaking, we can estimate the rate of ΣN formation as about one half of that of Λp . Next we demand that there is a collision with $\Sigma N \rightarrow \Lambda p$ conversion. The cross section for this reaction in the region of interest to us is of the order of 20 mb [42]. Using eq. (12) with $\rho = \rho_0/2$, since in the second part of eq. (14) the Λp conversion occurs only on neutrons or only on protons depending on the Σ charge, one obtains a survival

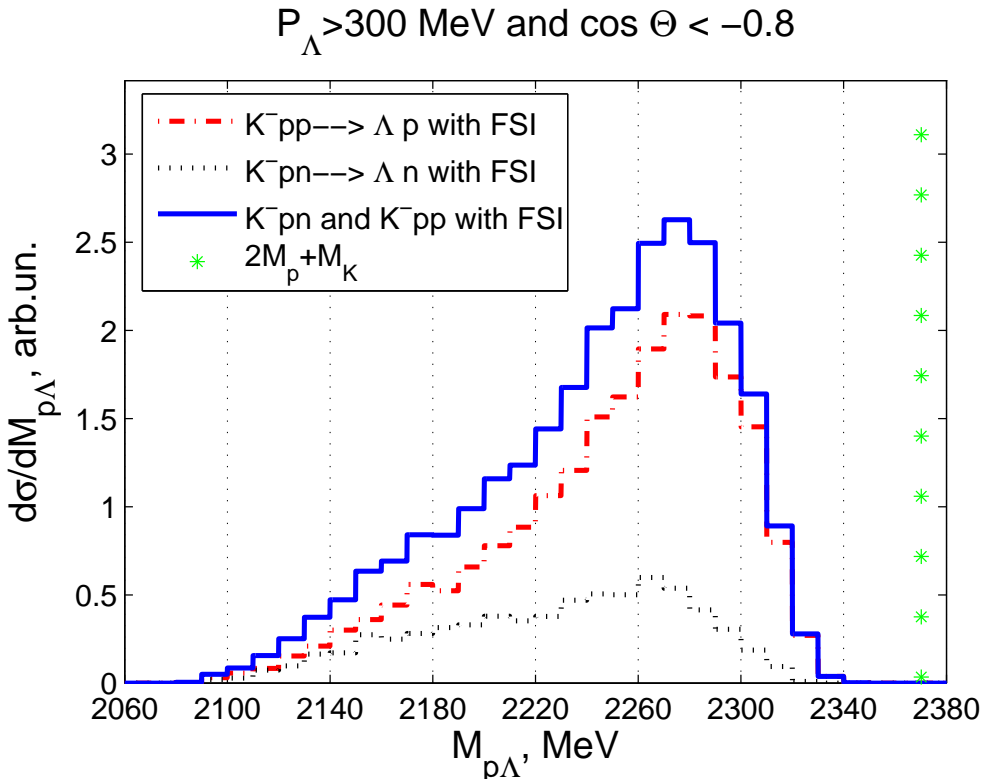


Figure 8: The same as Fig. 7, but imposing the experimental angle cut for back to back events, $\cos \Theta_{\vec{p}_\Lambda \vec{p}_p} < -0.8$.

probability of the order of 0.63 and, correspondingly, a 37 % probability for $\Sigma N \rightarrow \Lambda N$ conversion in the nucleus. All together, considering also the larger probability of NN or ΛN quasielastic collisions we find about one fourth of Λp events coming from this source compared to those from $K^- pp \rightarrow \Lambda p$ followed by Λ or p quasielastic collisions. However, when the Λ and p momenta in their CM frame are boosted to the rest frame of the nucleus where the Σ has about 450 MeV/c, the angle between the Λ and the p span a broad range and the fraction of events that fulfill the condition $\cos \Theta_{\vec{p}_\Lambda \vec{p}_p} < -0.8$ is very small. Together with the ratio one fourth of the events discussed above these contributions are negligible. That small fraction would peak in the region of $\sqrt{s} = 2170$ MeV, where indeed there is a little bump in Fig. 3 of [34].

One can also trace the, even fewer, events recombining the primary p from $K^- pp \rightarrow \Sigma^0 p$ with the Λ from $\Sigma N \rightarrow \Lambda N$ conversion. The same arguments also hold in this case and the angle cut constrain leaves a negligible amount of events from this mechanism to account for the spectrum of Fig. 3 of [34].

The discussion presented in this section on other possible sources of Λp pairs reinforces our conclusions that the spectrum shown in Fig. 3 of [34] comes essentially from $K^- pN \rightarrow \Lambda N$ absorption followed by further interaction of the N or the Λ with other nucleons, with a small and narrow contribution coming from the formation of the g.s. of the daughter nucleus.

6 Conclusions

In summary, we have seen that the Λp invariant mass distribution shown in Fig. 3 of [34] from K^- absorption in nuclei is naturally explained in terms of $K^-pN \rightarrow \Lambda N$ reaction followed by further interaction of the N or the Λ in the daughter nucleus. The events with one collision account for the big peak in Fig. 3 of [34], interpreted there as a signal of the formation of the K^-pp bound state. The bump at low invariant masses is accounted by events with two or more collisions. The small and narrow peak at higher invariant masses finds here the same interpretation as in [34], i.e. $K^-pp \rightarrow \Lambda p$ absorption leaving however the daughter nucleus in the ground state.

The explanation we have found has obvious experimental implications. Since the peak, claimed to be a signal for the K^-pp bound state, is associated in our interpretation to the $K^-pN \rightarrow \Lambda N$ absorption followed by final state interactions of the N or the Λ with nucleons in the daughter nucleus, it should not appear if we produce the Λp pairs in elementary reactions. On the contrary, according to the interpretation of [34], if the K^-pp system couples to Λp with such a large strength, so should the Λp system couple to the K^-pp state at the Λp invariant mass given by the main peak in Fig. 3 of [34], $\sqrt{s} = 2260$ MeV. Such invariant masses are easily reachable in the $pp \rightarrow K^+\Lambda p$ reaction at low energies. Although a devoted experiment for the present purpose has not been done, the present state of the art, with reactions like $pp \rightarrow K^+p\pi^-X^+$ being currently considered [43], indicate that the $pp \rightarrow K^+\Lambda p$ reaction is not particularly difficult, and its performance, looking at the Λp invariant mass, would be most instructive to further clarify the issue discussed here.

7 Acknowledgments

This work is partly supported by contracts BFM2003-00856 and FIS2005-03142 from MEC (Spain) and FEDER, the Generalitat de Catalunya contract 2005SGR-00343, and the E.U. EURIDICE network contract HPRN-CT-2002-00311. This research is part of the EU Integrated Infrastructure Initiative Hadron Physics Project under contract number RII3-CT-2004-506078.

References

- [1] H. Toki and T. Yamazaki, Phys. Lett. B **213** (1988) 129.
- [2] H. Toki, S. Hirenzaki, T. Yamazaki and R. S. Hayano, Nucl. Phys. A **501** (1989) 653.
- [3] J. Nieves, E. Oset and C. Garcia-Recio, Nucl. Phys. A **554** (1993) 509.
- [4] T. Yamazaki *et al.*, Z. Phys. A **355** (1996) 219.
- [5] K. Itahashi *et al.*, Phys. Rev. C **62** (2000) 025202.

- [6] H. Toki, S. Hirenzaki and T. Yamazaki, Nucl. Phys. A **530** (1991) 679.
- [7] S. Hirenzaki, H. Toki and T. Yamazaki, Phys. Rev. C **44** (1991) 2472.
- [8] C. J. Batty, E. Friedman and A. Gal, Phys. Rept. **287** (1997) 385.
- [9] E. Friedman and A. Gal, Phys. Lett. B **459** (1999) 43 [arXiv:nucl-th/9902036].
- [10] E. Friedman and A. Gal, Nucl. Phys. A **658** (1999) 345 [arXiv:nucl-th/9907052].
- [11] S. Hirenzaki, Y. Okumura, H. Toki, E. Oset and A. Ramos, Phys. Rev. C **61** (2000) 055205.
- [12] A. Baca, C. Garcia-Recio and J. Nieves, Nucl. Phys. A **673** (2000) 335 [arXiv:nucl-th/0001060].
- [13] V. Koch, Phys. Lett. B **337** (1994) 7 [arXiv:nucl-th/9406030].
- [14] M. Lutz, Phys. Lett. B **426** (1998) 12 [arXiv:nucl-th/9709073].
- [15] A. Ramos and E. Oset, Nucl. Phys. A **671** (2000) 481 [arXiv:nucl-th/9906016].
- [16] J. Schaffner-Bielich, V. Koch and M. Effenberger, Nucl. Phys. A **669** (2000) 153 [arXiv:nucl-th/9907095].
- [17] A. Cieply, E. Friedman, A. Gal and J. Mares, Nucl. Phys. A **696** (2001) 173 [arXiv:nucl-th/0104087].
- [18] Y. Akaishi and T. Yamazaki, Phys. Rev. C **65** (2002) 044005.
- [19] T. Suzuki *et al.*, Phys. Lett. B **597** (2004) 263.
- [20] Y. Akaishi, A. Dote and T. Yamazaki, Phys. Lett. B **613** (2005) 140 [arXiv:nucl-th/0501040].
- [21] M. Sato, talk at the Hadron Physics at COSY Workshop, Badhonnef (Germany), July 2005.
- [22] M. Sato, talk at the PANIC05 Santa Fe Conference, October 2005.
- [23] E. Oset and H. Toki, Phys. Rev. C, in print [arXiv:nucl-th/0509048].
- [24] E. Oset and A. Ramos, Nucl. Phys. A **635** (1998) 99 [arXiv:nucl-th/9711022].
- [25] J. A. Oller and U. G. Meissner, Phys. Lett. B **500** (2001) 263 [arXiv:hep-ph/0011146].
- [26] D. Jido, J. A. Oller, E. Oset, A. Ramos and U. G. Meissner, Nucl. Phys. A **725** (2003) 181 [arXiv:nucl-th/0303062].
- [27] B. Borasoy, R. Nissler and W. Weise, arXiv:hep-ph/0505239.

- [28] J. A. Oller, J. Prades and M. Verbeni, arXiv:hep-ph/0508081.
- [29] T. Hyodo, S. I. Nam, D. Jido and A. Hosaka, Phys. Rev. C **68** (2003) 018201 [arXiv:nucl-th/0212026].
- [30] S. Prakhov *et al.* [Crystall Ball Collaboration], Phys. Rev. C **70** (2004) 034605.
- [31] V. K. Magas, E. Oset and A. Ramos, Phys. Rev. Lett. **95** (2005) 052301 [arXiv:hep-ph/0503043].
- [32] J. Schaffner, C. B. Dover, A. Gal, C. Greiner and H. Stoecker, Phys. Rev. Lett. **71** (1993) 1328.
- [33] N. Grion and S. Piano, private communication. See preliminary results in the talk of T. Yamazaki at the chiral05 Conference, Tokyo, 2005, <http://chiral05.riken.jp/>
- [34] M. Agnello *et al.* [FINUDA Collaboration], Phys. Rev. Lett. **94** (2005) 212303.
- [35] A. Ramos, E. Oset, L.L. Salcedo, Phys. Rev. C50 (1994) 2314.
- [36] L. L. Salcedo, E. Oset, M. J. Vicente-Vacas and C. Garcia-Recio, Nucl. Phys. A **484** (1988) 557.
- [37] R. C. Carrasco, M. J. Vicente Vacas and E. Oset, Nucl. Phys. A **570** (1994) 701.
- [38] A. Gil, J. Nieves and E. Oset, Nucl. Phys. A **627** (1997) 599 [arXiv:nucl-th/9710070].
- [39] I. Vidaña, A. Polls, A. Ramos and H. J. Schulze, Phys. Rev. C **64**, 044301 (2001).
- [40] M. Preston and R.K. Bhaduri, Structure of the Nucleus, Addison-Wesley, 1975.
- [41] P. A. Katz, K. Bunnell, M. Derrick, T. Fields, L. G. Hyman and G. Keyes, Phys. Rev. D **1** (1970) 1267.
- [42] R. Engelman, H. Filthuth, V. Hepp and E. Kluge, Phys. Lett. **21**, 587 (1966); V. Hepp and M. Schleich, Z. Phys. **214**, 71 (1968); D. Stephen, Ph.D. Thesis, University of Massachusetts, 1970.
- [43] I. Zychor *et al.*, arXiv:nucl-ex/0506014, Phys. Rev. Lett., in print.